Flat-panel CT arthrography for cartilage defect detection in the ankle joint: first results in vivo

Sarah Pagliano, David Chemouni, Roman Guggenberger, Vanessa Pauly, Daphne Guenoun, Pierre Champsaur, Thomas Le Corroller

Flat-panel CT arthrography for cartilage defect detection in the ankle joint: first results in vivo

Pagliano Sarah [1,2] · Chemouni David [1] · Guggenberger Roman [3] · Pauly Vanessa [4] · Guenoun Daphné [1,2] · Champsaur Pierre [1,2] · Thomas Le Corroller [1,2]

Abstract

Objectives The purpose of this study was to compare the diagnostic performance of flat-panel computed tomography (FPCT) arthrography for cartilage defect detection in the ankle joint to direct magnetic resonance (MR) arthrography using multidetector computed tomography (MDCT) arthrography as the reference standard.

Methods Twenty-seven patients with specific suspicion of articular cartilage lesion underwent ankle arthrography with injection of a mixture of diluted gadolinium and iobitridol and were examined consecutively with the use of FPCT, MDCT, and 1.5 *T* MR imaging. FPCT, MDCT, and MR arthrography examinations were blinded and randomly evaluated by two musculoskeletal radiologists in consensus. In each ankle, eight articular cartilage areas were assessed separately: medial talar surface, medial talar trochlea, lateral talar trochlea, lateral talar surface, tibial malleolus, medial tibial plafond, lateral tibial plafond, and fibular malleolus. Findings at FPCT and MR were compared with MDCT assessments in 216 cartilage areas.

Results For the detection of cartilage defects, FPCT demonstrated a sensitivity of 97%, specificity of 95%, and accuracy of 96%; and MR arthrography showed a sensitivity of 69%, specificity of 94%, and accuracy of 87%. FPCT and MR arthrography presented almost perfect agreement ($\kappa = 0.87$) and moderate agreement ($\kappa = 0.60$), respectively, with MDCT arthrography. Mean diagnostic confidence was higher for FPCT (2.9/3) than for MR (2.3/3) and MDCT (2.7/3) arthrography.

Conclusions FPCT demonstrated better accuracy than did 1.5 *T* MR arthrography for cartilage defect detection in the ankle joint. Therefore, FPCT should be considered in patients scheduled for dedicated imaging of ankle articular cartilage.

Keywords Ankle · Arthrography · CT · MRI

Introduction

Chondral and osteochondral lesions related to traumatic injuries frequently occur at the ankle, where they represent the most important joint-related risk factors for osteoarthritis [1]. In most patients, clinical symptoms are nonspecific; and standard radiographs are known to be inaccurate for the evaluation of the articular cartilage status [2]. Because detection of cartilage defects in the ankle joint is crucial for surgical decision-making, many investigators have explored a variety of imaging techniques for assessing the integrity of hyaline cartilage [3–8].

Standard magnetic resonance (MR) imaging is commonly regarded the first-line cross-sectional imaging modality in patients presenting with post-traumatic ankle pain. Yet, articular cartilage in the ankle is particularly difficult to study with MR imaging, even at 3.0 Tesla (*T*) [8]. Direct MR arthrography leads to better results in the detection of chondral defects compared with standard MR imaging and should therefore be considered in patients with specific suspicion of articular cartilage lesion [3, 5, 8, 9].

On the other hand, in the past few years, improvements in computed tomography (CT) technology such as reduction of radiation dose and its wide availability have sparked a renewed interest in CT arthrography [10, 11]. Current detector designs in multidetector CT (MDCT) can reach a maximal z-

✉ Thomas Le Corroller
Thomas.LeCorroller@ap-hm.fr

[1] Radiology Department, APHM, Marseille, France

[2] CNRS, ISM UMR 7287, Aix-Marseille Université, Marseille, France

[3] Institute of Diagnostic and Interventional Radiology, University Hospital Zurich, Ramistrasse 100, 8091 Zurich, Switzerland

[4] Unité de Recherche EA3279, Santé Publique et Maladies Chroniques: Qualité de vie Concepts, Usages et Limites, Déterminants, Aix-Marseille Université, Marseille, France

resolution of 0.4–0.5 mm, enabling the detection of small cartilage and bone lesions that could be overlooked in MR arthrography [10, 11]. Thus, MDCT arthrography is considered the method of choice in the assessment of articular cartilage, especially in the ankle joint where hyaline cartilage is particularly thin [3, 6, 7, 12].

Furthermore, modern fluoroscopy units equipped with C-arm and digital flat-panel detector technology can provide a volumetric dataset suitable for multiplanar reformations similar to that obtained with MDCT. By automatic rotation of the C-arm around the object and acquisition of a predefined number of 2D projections, flat-panel CT (FPCT) offers ultra-high spatial resolution with isotropic voxel sizes as small as 0.15 mm [13, 14]. Other advantages of FPCT include its large volumetric coverage and reduced metal and beam-hardening artifacts [15, 16]. FPCT arthrography has recently been shown to be as feasible as MDCT arthrography with similar image quality in vitro and ex vivo [7, 13, 14, 17]. In clinical practice, FPCT arthrography can now be performed immediately after arthrography, without relocating the patient, which avoids resorption of contrast material and improves workflow [18, 19]. However, FPCT arthrography is a relatively new imaging modality that has mostly been studied on phantoms and cadaveric specimens, with very limited in vivo evaluation [7, 13, 14, 17–19].

Thus, the purpose of this study was to prospectively compare the diagnostic performance of FPCT arthrography for detecting cartilage defects in the ankle joint to direct 1.5 *T* MR arthrography using MDCT arthrography as the reference standard.

Materials and methods

Patients

Twenty-seven patients were prospectively enrolled between July 2015 and April 2017. Inclusion criteria were suspicion of articular cartilage lesion of the ankle joint with proposed arthroscopic treatment and FPCT, MDCT, and MR arthrography of the ankle performed on the same day in our institution as part of the preoperative work-up. Exclusion criteria were a history of previous ankle arthroscopy or open surgery and a time delay between contrast agent injection and cross-sectional imaging longer than 30 min. Fifteen patients were male and 12 were female. The age range was 14–76 years (mean age, 37 years). All patients were informed that their charts could be reviewed for scientific purposes and gave their informed consent. The institutional ethics committee approved the study.

Contrast injection

Ankle arthrography was performed under fluoroscopic guidance and sterile conditions using a 22 *G* needle with an anterior approach lateral to the dorsalis pedis artery. Intra-articular positioning of the needle was confirmed by injection of a small amount of iodinated contrast. This was followed by injection of 5 cc of a 1:1 mixture of an iodinated contrast agent (iobitridol 300 mg/mL, Xenetix, Guerbet) and a pre-diluted gadolinium-based contrast agent (gadolinium-DTPA 2 mmol/L, Magnevist, Bayer). After injection, the ankle was passively moved to ensure homogenous distribution of the contrast agent within the joint cavity.

Imaging technique

Immediately after intra-articular contrast injection, FPCT scans were performed on the same angiographic unit (Allura FD 20, Philips Healthcare) with a C-arm-mounted flat-panel detector. Detector size was 30 × 40 cm. An 8 s run protocol was used with a 180° rotation of the C-arm around the object. The distance from the source to the object was 120 cm. FOV was 22 cm. This resulted in a spatial resolution of isotropic raw-images of 0.15 mm. A vendor-specific tube voltage of 80 kV was used. Tube current-time product was determined automatically, with a mean of 86 mAs.

Then, MDCT acquisitions were performed on a 64-MDCT unit (LightSpeed VCT 64, GE Healthcare) using the standard protocol for ankle arthrography (120 kV, 160 mAs, FOV of 11.5 cm, slice thickness of 0.625 mm, reconstruction interval of 0.625 mm, focal spot length of 0.7 mm, pitch of 0.5, 512 × 512 matrix, and bone reconstruction kernel). Multiplanar reformations were calculated from raw data in coronal, sagittal, and axial planes for both FPCT and MDCT. Slice thickness (1 mm) and increment (0.6 mm) were identical.

Finally, within 30 min after contrast injection, MR imaging was performed on a 1.5-*T* unit (Achieva, Philips Healthcare) using a dedicated 8-channel ankle coil. The following sequences were obtained in every patient: sagittal T1-weighted turbo spin-echo (SE) (TR/TE 561/20; FOV 240 mm; slice thickness 3.5 mm; matrix 512 × 512), coronal T1-weighted fat-suppressed (FS) SE (TR/TE 566/20; FOV 150 mm; slice thickness 3.5 mm; matrix 512 × 512), axial T1-weighted FS SE (TR/TE 517/14; FOV 160 mm; slice thickness 3 mm; matrix 512 × 512), and 3D spectral attenuated inversion recovery (SPAIR) proton-density (TR/TE 800/35; FOV 160 mm; slice thickness 0.5 mm; matrix 512 × 512). Multiplanar reformations were calculated from 3D data in coronal, sagittal, and axial planes, using a slice thickness of 1 mm and increment of 0.6 mm to facilitate comparison with analogous FPCT and MDCT 1 mm-thick reformatted images. Here note that because the standard ankle MR arthrography protocol classically employs sagittal, coronal, and axial acquisitions, we have performed complete assessment of the three planes T1SE sequences in addition to the 1 mm-thick proton-density FS reformatted images when the reading of the MR examinations was made.

Imaging analysis

FPCT, MDCT, and MR examinations were blinded and randomly evaluated using a dedicated workstation (AW Volume Share 2, GE Healthcare). Two radiologists with respectively 12 and 3 years of experience in musculoskeletal imaging interpreted the imaging data in consensus. Readings between the FPCT, MDCT, and MRI examinations were each time separated by a 4-week interval.

First, delineation of articular cartilage, defined as a continuous contrast layer between the two cartilage surfaces, was judged as satisfactory or not for each acquisition.

Then, as previously suggested by Chemouni et al., eight anatomical areas were assessed separately in each ankle examination: medial talar surface (pear-shaped articular facet for articulation with the tibial malleolus), medial talar trochlea (medial half of the superior surface of the talar body for articulation with the tibial plafond), lateral talar trochlea (lateral half of the superior surface of the talar body for articulation with the tibial plafond), lateral talar surface (large triangular facet for articulation with the fibular malleolus), tibial malleolus, medial tibial plafond, lateral tibial plafond, and fibular malleolus [7]. Each of these eight anatomical regions was graded as either normal or presenting a cartilage defect. Cartilages defects were defined by the penetration of contrast material within the cartilage.

Finally, for each acquisition, a confidence level between 1 and 3 (1, low confidence indicating that a diagnosis is hardly possible; 2, moderate confidence indicating that a diagnosis can be made but with uncertainty; and 3, high confidence indicating that a diagnosis can be made unequivocally) was attributed to each diagnosis as previously described by Schmid et al. [3].

Statistical analysis

Data analysis was performed by a statistician. Continuous variables were described by their mean and range, and qualitative variables by their count and proportion.

Sensitivity, specificity, and accuracy values for detecting cartilage defects were calculated for FPCT and MR arthrography using MDCT arthrography as the reference standard. All percentages were calculated with a 95% confidence interval.

The McNemar's test was performed to determine whether the diagnostic performance of FPCT and MR arthrography differed significantly from the results provided by the MDCT arthrography. In addition, the reliability of FPCT and MR arthrography in accurately identifying the cartilage defects diagnosed with MDCT arthrography was assessed using the kappa statistic, which was interpreted as follows: kappa values of 0.20 or less indicate poor agreement, kappa values of 0.21–0.40 indicate fair agreement, kappa values of 0.41–0.60 indicate moderate agreement, kappa values of 0.61–0.80 indicate good agreement, and kappa values of 0.81–1.00 indicate very good agreement.

The Mann-Whitney *U* test was used to determine whether the confidence levels differed significantly between FPCT, MR, and MDCT acquisitions. A p value of less than 0.05 was considered statistically significant. Statistical analysis was performed using SPSS for Windows (version 15.0, SPSS).

Results

Complete delineation of articular cartilage, defined as a continuous contrast layer between the two cartilage surfaces, was judged satisfactory in respectively 100% MDCT arthrography (27/27), 96% FPCT arthrography (26/27), and 78% MR arthrography (21/27) examinations (Fig. 1).

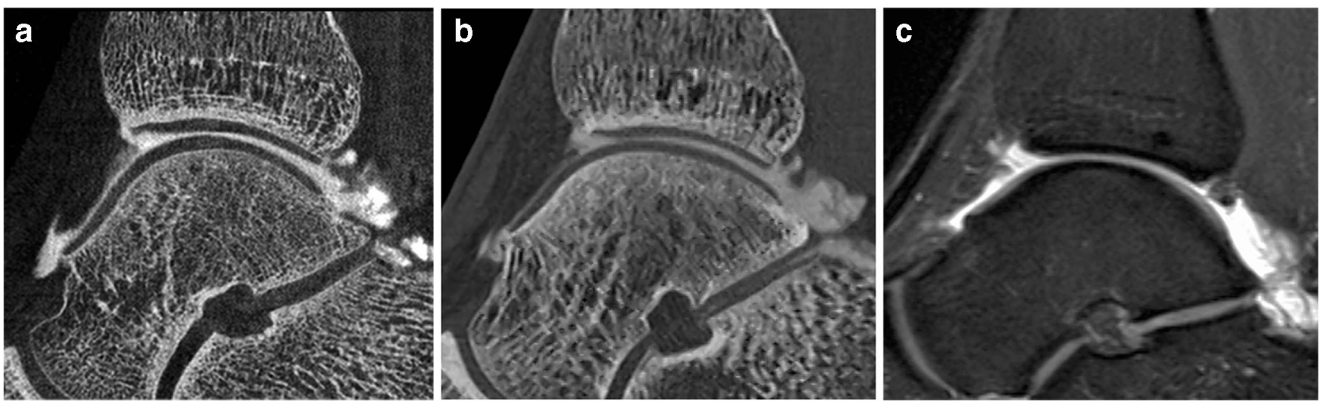

Fig. 1 Sagittal reformatted images demonstrating delineation of articular cartilage, defined as a continuous contrast layer between the two cartilage surfaces, obtained respectively with FPCT (Fig. 1a), MDCT (Fig. 1b), and MR (Fig. 1c) arthrography. Note that complete delineation of articular cartilage is suboptimal on MR image in comparison with FPCT and MDCT

Table 1 Diagnostic performance of FPCT and MR arthrography in the detection of cartilage defects with MDCT arthrography as standard of reference

Region	*Areas with cartilage defects (no./total)*	*Flat-panel CT arthrography*			*MR arthrography*		
		Se	Sp	Acc	Se	Sp	Acc
All regions	64/216	97 (62/64)	95 (145/152)	96 (207/216)	69 (44/64)	94 (143/152)	87 (187/216)
Talus							
Medial talar surface	5/27	100 (5/5)	100 (22/22)	100 (27/27)	80 (4/5)	100 (22/22)	96 (26/27)
Medial talar trochlea	13/27	100 (13/13)	100 (14/14)	100 (27/27)	69 (9/13)	100 (14/14)	85 (23/27)
Lateral talar trochlea	10/27	90 (9/10)	88 (15/17)	89 (24/27)	60 (6/10)	94 (16/17)	81 (22/27)
Lateral talar surface	5/27	100 (5/5)	100 (22/22)	100 (27/27)	40 (2/5)	100 (22/22)	89 (24/27)
Tibia							
Tibial malleolus	4/27	100 (4/4)	100 (23/23)	100 (27/27)	75 (3/4)	96 (22/23)	93 (25/27)
Medial tibial plafond	10/27	90 (9/10)	76 (13/17)	81 (22/27)	90 (9/10)	71 (12/17)	78 (21/27)
Lateral tibial plafond	13/27	100 (13/13)	93 (13/14)	96 (26/27)	69 (9/13)	86 (12/14)	78 (21/27)
Fibula							
Fibular malleolus	4/27	100 (4/4)	100 (23/23)	100 (27/27)	50 (2/4)	100 (23/23)	93 (25/27)

Note—data are percentages. Numbers in parentheses are raw data

Se sensitivity; *Sp* specificty; *Acc* accuracy

At MDCT arthrography, 64 regions with cartilage defects and 152 areas of normal articular cartilage were observed (Table 1).

With MDCT arthrography as the standard of reference, FPCT arthrography showed a sensitivity of 97% (62/64), specificity of 95% (145/152), and accuracy of 96% (207/216); and MR arthrography showed a sensitivity of 69% (44/64), specificity of 94% (143/152), and accuracy of 87% (187/216), for the detection of articular cartilage defects (Table 1). The diagnostic performance of MR arthrography differed significantly from the results provided by the reference standard ($p < 0.001$), whereas that of FPCT arthrography did not ($p > 0.05$).

FPCT and MR arthrography presented respectively almost perfect agreement ($\kappa = 0.87$) and moderate agreement ($\kappa = 0.60$) with MDCT arthrography (Table 2).

The confidence levels attributed to each diagnosis between 1 and 3 were for FPCT 1 (0%), 2 (11.1%), and 3 (88.9%); for MDCT 1 (0%), 2 (29.6%), and 3 (70.4%); and for MR 1 (3.7%), 2 (63%), 3 (33.3%). The mean diagnostic confidence, on a scale of 1 to 3, was higher for FPCT (2.9/3) than for MR (2.3/3) and MDCT (2.7/3) arthrography. The difference between confidence levels of FPCT arthrography and MR arthrography was statistically significant ($p = 0.001$), whereas the difference between FPCT and MDCT arthrography was not ($p > 0.05$).

Table 2 Reliability of FPCT and MR arthrography in the detection of cartilage defects

Region	FPCT arthrography reliability[a] (κ)	MR arthrography reliability[a] (κ)
All regions	0,873	0,604
Talus		
Medial talar surface	0,884	0,621
Medial talar trochlea	0,878	0,669
Lateral talar trochlea	0,799	0,619
Lateral talar surface	0,883	0,376
Tibia		
Tibial malleolus	1	0,574
Medial tibial plafond	0,683	0,507
Lateral tibial plafond	0,941	0,627
Fibula		
Fibular malleolus	1	0,453

Note—[a] defined as agreement with MDCT arthrography

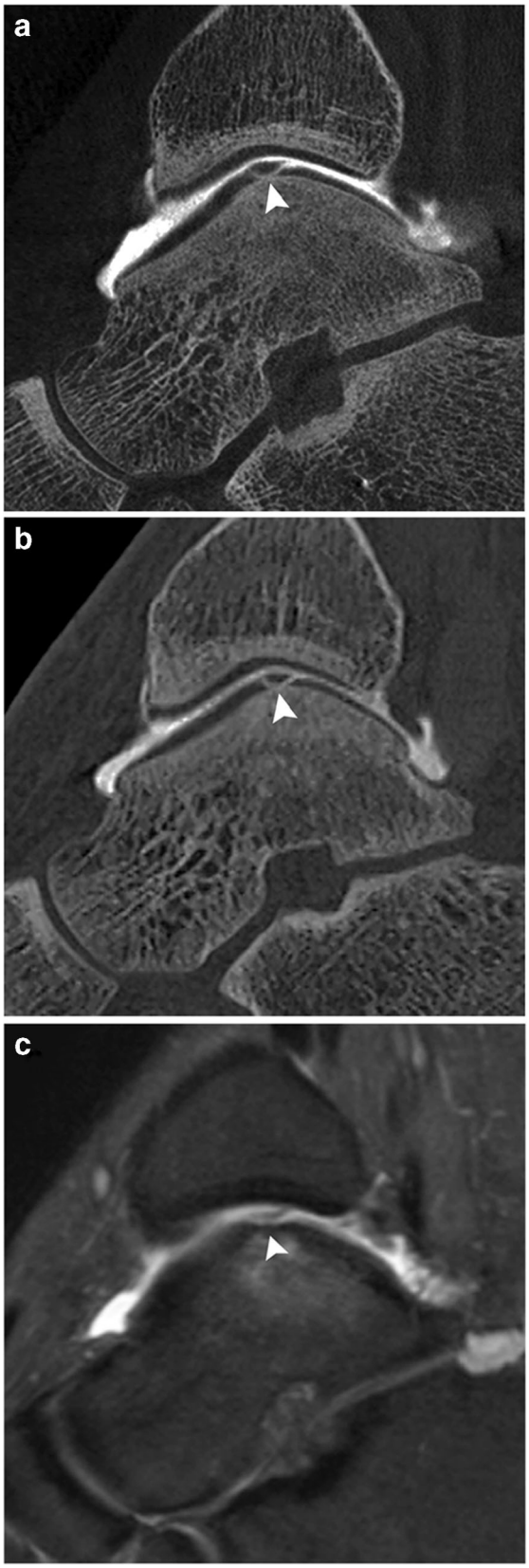

Fig. 2 Sagittal reformatted FPCT (Fig. 2a), MDCT (Fig. 2b), and MR (Fig. 2c) arthrography images exhibiting a chondral flap of the talar dome (arrowhead). Of note, MR image allows detection of cartilage defect but does not permit fine assessment of the flap

Discussion

Because current surgical treatment paradigms aim at restoring the articular surface with a repair tissue similar to native cartilage, the preoperative assessment of hyaline cartilage in the ankle joint is important for precise localization of cartilage defects before planning surgical access and for determination of cartilage surface damage in osteochondral lesions to plan the type of surgical procedure [1, 2, 20].

Direct MR arthrography has classically been considered the method of choice for assessing internal joint derangement and cartilage integrity [21, 22]. On the other hand, CT arthrography offers an alternative to MR arthrography, capable of isotropic data acquisition with high spatial resolution, and may routinely be used for cartilage imaging [6, 7, 12]. Recently, an innovative CT scanner design providing volumetric imaging with ultra-high spatial resolution consists in the use of digital flat-panel detectors [23]. Hence, FPCT can provide exquisite spatial resolution, up to 150 × 150 μm, and may have the potential to outperform MDCT in CT arthrography [7, 13]. In addition, at the ankle, the radiation dose in FPCT is usually similar to or even lower than that associated with MDCT if optimized collimation and scan parameters are used [7]. However, FPCT arthrography is a relatively new imaging modality that remains poorly investigated in vivo [18, 19].

In the present study, we compared FPCT and 1.5 *T* MR arthrography for detecting cartilage lesions in the ankle joint of patients with specific suspicion of chondral lesion. We found that FPCT arthrography was superior to MR arthrography in diagnosing articular cartilage defects. Our results are in line with previous studies, suggesting that FPCT arthrography permits fine assessment of articular cartilage [7, 13, 14]. In the same way, Sonnow et al. recently showed that FPCT arthrography of the wrist is advantageous over 3 *T* MR arthrography regarding the depictability of the intrinsic ligaments, TFCC, and hyaline cartilage [19]. Given its higher spatial resolution, FPCT arthrography logically offers better delineation of articular cartilage lesions than MR arthrography, especially in the ankle joint where hyaline cartilage is very thin. Furthermore, we noted that FPCT provided excellent assessment of chondral flaps at the ankle, which is of particular importance for the preoperative planning (Fig. 2). We also observed in specific cases that FPCT allowed excellent evaluation of the osteochondral lesions of the talar dome and provided exquisite assessment of the os trigonum and of the talar interface with the fragment (Fig. 3). Finally, in our study, FPCT acquisition could easily be combined with MR arthrography, immediately following the intra-articular contrast injection and prior to MR examination, in order to obtain not only excellent depiction of soft tissue and bone marrow injuries with MR imaging but also exquisite articular cartilage assessment.

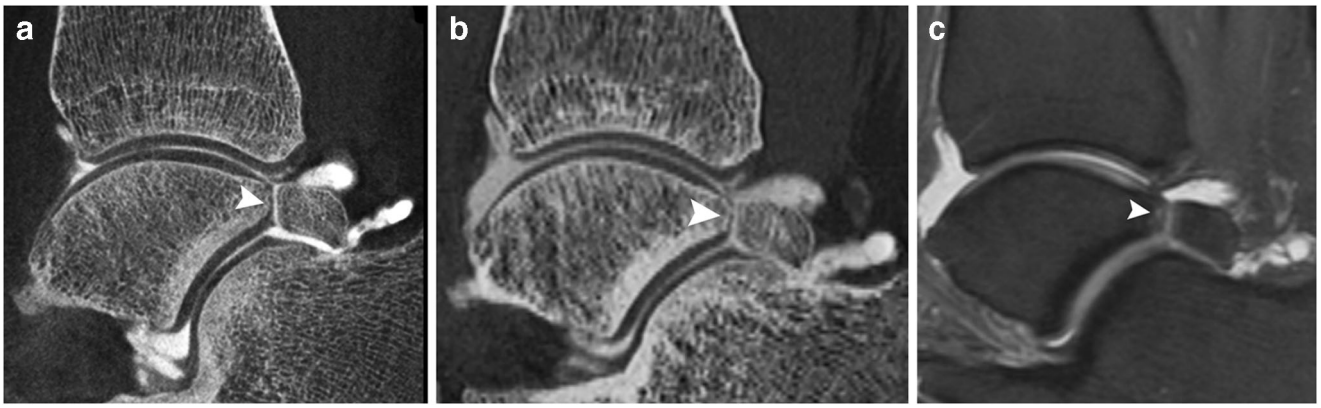

Fig. 3 Sagittal reformatted FPCT (Fig. 3a), MDCT (Fig. 3b), and MR (Fig. 3c) arthrography images showing an os trigonum with disruption of its attachment to the talus. FPCT image provides excellent assessment of the talar interface with the fragment (arrowhead)

Some limitations inherent to the materials and methods used in our study should now be considered. First, FPCT arthrography is an innovative technique that has mostly been studied on phantoms, animals, or using cadaveric specimens, with very limited in vivo evaluation [7, 13, 14, 17–19]. Second, we acknowledge that the use of different FPCT acquisition protocols, with different scan duration, tube voltage, and current, may lead to lower contrast-to-noise ratio, or to increased radiation dose, than that observed in our study [7]. Third, compared with 3 *T* MR imaging, the use of 1.5 *T* MR arthrography may have lead in our study to decreased spatial resolution and lower diagnostic performance in assessing articular cartilage. Then, because all FPCT, MDCT, and MR arthrography examinations were analyzed by two radiologists in consensus, we did not specifically assess or compare the interobserver variation of each imaging modality. Finally, another limitation of our study is the lack of comparison to diagnostic arthroscopy. In our population, the number of patients that indeed received a subsequent arthroscopy within 3 months after imaging was insufficient for an appropriate statistical analysis. Yet, because the field of view during ankle arthroscopy is limited, the value of arthroscopy reports as a standard of reference should not be overestimated [3].

In conclusion, in our study, FPCT arthrography demonstrated better accuracy than did 1.5 *T* MR arthrography for cartilage defect detection in the ankle joint. In addition, we noted that, because contrast agent injection and cross-sectional imaging can be performed without any delay and without patient transfer, FPCT acquisition optimizes workflow and may, even if necessary, easily be combined with MR imaging, in order to obtain both excellent depiction of soft tissue and bone marrow injuries, and exquisite articular cartilage assessment. Therefore, FPCT arthrography should now be considered in patients scheduled for dedicated imaging of ankle articular cartilage.

Compliance with ethical standards

Conflict of interest The authors declare that they have no conflict of interest.

Ethical approval The institutional ethics committee approved the study.

References

1. Johnson VL, Giuffre BM, Hunter DJ. Osteoarthritis: what does imaging tell us about its etiology? Semin Musculoskelet Radiol. 2012;16(5):410–8.
2. O'Loughlin PF, Heyworth BE, Kennedy JG. Current concepts in the diagnosis and treatment of osteochondral lesions of the ankle. Am J Sports Med. 2010;38:392–404.
3. Schmid MR, Pfirrmann CW, Hodler J, Vienne P, Zanetti M. Cartilage lesions in the ankle joint: comparison of MR arthrography and CT arthrography. Skelet Radiol. 2003;32:259–65.
4. El-Khoury GY, Alliman KJ, Lundberg HJ, Rudert MJ, Brown TD, Saltzman CL. Cartilage thickness in cadaveric ankles: measurement with double contrast multi-detector row CT arthrography versus MR imaging. Radiology. 2004;233:768–73.
5. Cerezal L, Llopis E, Canga A, Rolon A. MR arthrography of the ankle: indications and technique. Radiol Clin N Am. 2008;46:973–94.
6. Kraniotis P, Maragkos S, Tyllianakis M, Petsas T, Karantanas AH. Ankle post-traumatic osteoarthritis: a CT arthrography study in patients with bi- and trimalleolar fractures. Skelet Radiol. 2012;41:803–9.
7. Chemouni D, Champsaur P, Guenoun D, Desrousseaux J, Pauly V, Le Corroller T. Diagnostic performance of flat-panel CT arthrography for cartilage defect detection in the ankle joint: comparison with MDCT arthrography with gross anatomy as the reference standard. AJR Am J Roentgenol. 2014;203:1069–74.
8. Bauer JS, Barr C, Henning TD, Malfair D, Ma CB, Steinbach L, et al. Magnetic resonance imaging of the ankle at 3.0 Tesla and 1.5 Tesla in human cadaver specimens with artificially created lesions of cartilage and ligaments. Invest Radiol. 2008;43:604–11.
9. Notohamiprodjo M, Kuschel B, Horng A, et al. 3D-MRI of the ankle with optimized 3D-SPACE. Investig Radiol. 2012;47:231–9.
10. Acid S, Le Corroller T, Aswad R, Pauly V, Champsaur P. Preoperative imaging of anterior shoulder instability: diagnostic

effectiveness of MDCT arthrography and comparison with MR arthrography and arthroscopy. AJR Am J Roentgenol. 2012;198: 661–7.
11. Omoumi P, Rubini A, Dubuc JE, Vande Berg BC, Lecouvet FE. Diagnostic performance of CT-arthrography and 1.5T MR-arthrography for the assessment of glenohumeral joint cartilage: a comparative study with arthroscopic correlation. Eur Radiol. 2015;25:961–9.
12. Jung HG, Kim NR, Jeon JY, Lee DO, Eom JS, Lee JS, et al. CT arthrography visualizes tissue growth of osteochondral defects of the talus after microfracture. Knee Surg Sports Traumatol Arthrosc. 2018;26:2123–30.
13. Guggenberger R, Fischer MA, Hodler J, Pfammatter T, Andreisek G. Flat-panel CT arthrography: feasibility study and comparison to multidetector CT arthrography. Investig Radiol. 2012;47:312–8.
14. Guggenberger R, Winklhofer S, Spiczak JV, Andreisek G, Alkadhi H. In vitro high-resolution flat-panel computed tomographic arthrography for artificial cartilage defect detection: comparison with multidetector computed tomography. Investig Radiol. 2013;48:614–21.
15. Gupta R, Grasruck M, Suess C, et al. Ultra-high resolution flat-panel volume CT: fundamental principles, design architecture, and system characterization. Eur Radiol. 2006;16:1191–205.
16. Gupta R, Cheung AC, Bartling SH, et al. Flat-panel volume CT: fundamental principles, technology, and applications. RadioGraphics. 2008;28:2009–22.
17. Guggenberger R, Morsbach F, Alkadhi H, et al. C-arm flat panel CT arthrography of the wrist and elbow: first experiences in human cadavers. Skelet Radiol. 2013;42:419–29.
18. Guggenberger R, Ulbrich EJ, Dietrich TJ, et al. C-arm flat-panel CT arthrography of the shoulder: Radiation dose considerations and preliminary data on diagnostic performance. Eur Radiol. 2017;27: 454–63.
19. Sonnow L, Koennecker S, Luketina R, et al. High-resolution flat panel CT versus 3.0 T MR arthrography of the wrist: initial results in vivo. Eur Radiol. 2019;29(6):3233–40.
20. Murawski CD, Kennedy JG. Operative treatment of osteochondral lesions of the talus. J Bone Joint Surg Am. 2013;95:1045–54.
21. Elentuck D, Palmer WE. Direct magnetic resonance arthrography. Eur Radiol. 2004;14:1956–67.
22. Cerezal L, Abascal F, García-Valtuille R, Canga A. Ankle MR arthrography: how, why, when. Radiol Clin N Am. 2005;43:693–707.
23. Reichardt B, Sarwar A, Bartling SH, et al. Musculoskeletal applications of flat-panel volume CT. Skeletal Radiol. 2008;37:1069–76.